Journal of Undergraduate Chemistry Research, **2020**,19(3), 8

GLUCOSE DECREASES THE ACTIVITY COEFFICIENT OF HYDROXIDE ANION: EFFECTS ON pH, pK_a AND ENZYME ACTIVITY pH PROFILE

Todd P. Silverstein† and Joshua D. Bumgarner*

Chemistry Department, Willamette University, Salem, OR 97301

Abstract

Crowding caused by macromolecular solutes (e.g., proteins, polysaccharides, oligonucleotides) has two different effects on probe solutes: excluded volume favors more compact structures, and chemical interactions favor the entity that is most strongly attracted to the crowding agents. These interactions can be distinguished by comparing the effects of a large, polymeric crowding agent (e.g., dextran) with its monomeric unit (e.g., glucose). We found that glucose did not alter the pK_a of two different small acids (acetic acid and bromophenol blue), but it did cause pH to fall by dramatically decreasing the activity coefficient of the hydroxide anion. In studies on yeast alcohol dehydrogenase (YADH), we found that glucose, dextran, and bovine serum albumin (BSA) all inhibited the enzyme and broadened its pH profile, increasing $pK_{a,hi}$, while leaving $pK_{a,lo}$ unchanged. The fact that glucose and dextran had similar effects rules out excluded volume as a causative factor. Instead, the effects of glucose, dextran, and BSA stem from chemical interactions and/or viscosity increase, with serum albumin's effect on $pK_{a,hi}$ being especially significant. BSA also enhanced YADH activity below pH 7.

† corresponding author: tsilvers@willamette.edu

*present address: Chemistry Dept., University of California, Davis, CA 95616

Keywords: pH and pK_a, molecular crowding, enzyme pH profile

Introduction

Biochemical reactions are usually studied in vitro, in dilute buffered solutions of purified molecules of interest. However, such experiments ignore the effects of macromolecular crowding in vivo. Cellular milieu include thousands of different types of macromolecules (proteins, oligonucleotides, polysaccharides, and membranes) that occupy 25 – 40% of the volume (1,2). These macromolecular crowding agents alter the stability of probe solutes in two ways: Their excluded volume has an entropic effect that favors more compact structures, and their enthalpic chemical interactions with the probe (e.g., charge-charge, hydrogen bonding, hydrophobic) can be attractive or repulsive. Recent reviews have summarized great strides made in this field (3-6).

In the cytoplasm, the most common crowding agents are proteins, followed by polysaccharides (1,2). Thus the most biologically relevant crowding agent to test experimentally would be a protein, e.g., bovine serum albumin (BSA) or lysozyme. At high concentrations, however, protein crowders can denature and aggregate, and even if they don't, they can overwhelm the signal from the probe protein. For this reason, polysaccharides like dextran (a glucose polymer) and Ficoll (a sucrose polymer) are often used to study the effects of crowding in vitro; these are commercially available in a wide range of sizes. In order to distinguish excluded volume effects from chemical interactions, the influence of the polymer (e.g., dextran) can be compared to that of the monomer (e.g., glucose), which does not exclude volume due to its small size. Any change caused by both stems from a chemical interaction, whereas a change caused by the polymer alone must be due to excluded volume (3).

Most experiments in this field have examined how macromolecular crowding influences protein folding and stability, ligand binding, and enzyme activity (3,4). Because effects on simple acid equilibria have so far not been addressed in the literature, we set out to study how crowding agents might alter pH and pK_a. As the H^+ and OH^- ions are quite small, we did not expect crowding to alter pH, unless chemical interactions are significant. The same is true of pK_a, unless deprotonation causes a dramatic change in size or shape. Accordingly, we titrated two acids and an enzyme in the presence of dextran, glucose, and BSA.

The enzyme that we chose to study was alcohol dehydrogenase from yeast (YADH, EC 1.1.1.1, UniProt # P00330) (7-9). YADH is a metalloenzyme in which an active site Zn^{2+} binds (and helps to deprotonate) its alcohol substrate. The enzyme also has a nucleotide binding domain that binds the NAD^+ oxidizing agent, after which a hydride anion is transferred from the alcohol C-H to NAD^+, as depicted in Scheme 1:

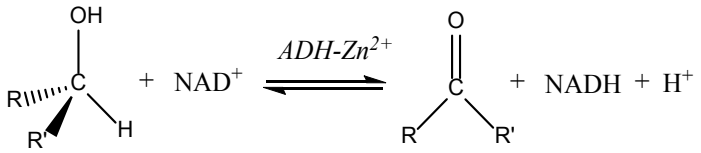

Scheme 1

Conveniently, the NADH product is a reasonably strong near-UV chromophore (ε_{340} = 6220 $M^{-1}cm^{-1}$). From its activity pH profile (7) we know that YADH has at least two catalytically important acidic groups, one with a pK_a of 7.5 that must be deprotonated to activate the enzyme, and another with a pK_a of 10.6 that is protonated in the active enzyme. As a result, the optimal pH for YADH activity is 9.1 (7).

Experimental Procedures

Spectrophotometric Titration of Bromophenol Blue

To a 50 mL beaker, 10.00 mL of 0.150 M bromophenol blue (CAS # 62625-28-9, from Sigma-Aldrich) was added. The solution was acidified to pH ≈ 1 with 0.5 M HCl, with mixing, and a 1.00 mL aliquot was transferred from the beaker to a semi-micro quartz cuvette. pH was measured with a Thermo Scientific Orion Star pH meter (model A211) and a standard pH electrode calibrated with three Sigma-Aldrich reference buffers: pH 4.01, 7.00, and 10.01. Absorbance was measured with a Cary 3 UV-vis spectrophotometer at 593 nm and 435 nm, the absorbance maxima of the bromophenol blue acid (yellow) and its blue conjugate base, respectively. With successive aliquots of 1 M NaOH, the pH in the beaker was increased up to 12, and after each pH adjustment, an aliquot was transferred to the quartz cuvette for absorbance measurement, as above. This process was repeated

using bromophenol blue solutions containing glucose at 200 and 400 g/L. Absorbance vs. pH data were fit to Equation 1 (A_{593}) and Equation 2 (A_{435}).

Standard Titration of Acetic Acid

In a 100 mL beaker, 15.00 mL of 13.3 mM acetic acid (i.e., 0.200 mmol) was placed. The buret was loaded with 20.00 mM NaOH, and aliquots of 2.5 – 5 mL were added to the gently stirred (to minimize CO_2 dissolution) beaker until the pH ceased to increase appreciably. pH was measured after each aliquot addition. The process was repeated for solutions that included 50, 100, 150, and 200 g/L of glucose (in both the beaker and the buret, to maintain constant concentration). pH vs. added OH^- (mmol) data were fit to Equation 3 up to the equivalence point, and to Equation 4 for the points at the end of the titration.

Glucose Effect on pH

A 25.00 mL portion of the acid or base to be tested (10, 100, 1000 µM HCl; 10, 50, 100, 1000 µM NaOH; 1 mM acetic acid) was added to a 100 mL beaker. For the acetic acid titration only, the initial pH was adjusted to the middle of its buffer zone, pH 4.75. To the buret was added a solution that contained both concentrated glucose (400 g/L) and the acid or base to be tested (so as not to alter its concentration during the titration). Initial pH was measured, after which glucose aliquots of about 5 mL were added to the gently stirred beaker, and pH was measured after each aliquot addition. Each titration was repeated at least twice, and pH values were averaged.

YADH Activity pH Profile

Each YADH activity assay was conducted by measuring the increase in A_{340} (from NADH) in a semi-micro UV-transparent plastic cuvette (1.00 cm path length). Each 1.00 mL sample contained: 250 µL of 1.00 mM NAD^+ (final concentration 0.250 mM; CAS# 53-84-9, from Sigma-Aldrich); 150 µL of 1.0 M ethanol (final concentration 150 mM); 100 µL of 0.2 M buffer (final concentration 20 mM; see Table S1 for the pH 4 – 13 buffers used); and 495 µL of deionized water. The Parafilm-covered cuvette was inverted several times to mix, then 5 µL of 0.50 mg/mL YADH (Sigma A-7011, EC 1.1.1.1) in 0.05 % (w/v) BSA was added, and the covered cuvette was quickly inverted again and loaded into a Genesis-500 UV-vis spectrophotometer for absorbance measurement; A_{340} was collected at 1 s intervals for at least 30 s. The slope of the initial linear absorbance vs. time data ($\Delta A_{340}/\Delta t$) was calculated, and then converted to v_0 in µM/s by dividing by 6220 M^{-1}. If the initial $\Delta A_{340}/\Delta t$ for the control YADH at pH 9 was < 0.12 min^{-1}, then the enzyme concentration was increased for that day's work. v_0 vs. pH data were fit to Equation 6.

The YADH pH profile in the presence of crowding agents was performed by replacing portions of the water aliquot with concentrated stock solution of crowder: 800 g/L glucose, 400 g/L dextran-40 (≈ 40 kDa, from Leuconostoc spp., CAS# 9004-54-0, Sigma-Aldrich), or 200 g/L BSA (CAS# 9048-46-8, 96% purity, from Sigma-Aldrich). The volume of the added crowder stock solution was adjusted to give final concentrations of 100, 200, 300, and 396 g/L glucose; 50, 100, 150, and 198 g/L dextran-40; and 25, 50, 75, and 98 g/L BSA. For each crowder concentration, v_0 vs. pH data were fit as above.

Results:

Effects of Glucose on Acid Titrations

The pH indicator bromophenol blue changes color from yellow to blue as the pH rises above 3. The two forms have λ_{max} values of 593 nm (deprotonated/blue) and 435 nm (protonated/yellow), so adding NaOH to an acidified 0.15 mM solution of bromophenol blue allowed us to create spectrophotometric titration curves (Figure 1). Absorbance vs. pH data were fit to the following versions of the Henderson-Hasselbalch equation:

$$A_{593}(B{:}^-) = \frac{\varepsilon_{593} \cdot c_0}{(1 + 10^{(pK_a - pH)})} \quad (1)$$

$$A_{435}(BH) = \frac{\varepsilon_{435} \cdot c_0}{(1 + 10^{(pH - pK_a)})} \quad (2)$$

where c_0 is the initial (i.e., total) concentration of acid, in this case, 0.15 mM.

It is clear from Figure 1 that at least up to 400 g/L (2.2 M), glucose has no effect on the pK_a of bromophenol blue. All points for the three titrations (0, 200, and 400 g/L glucose) lie on the

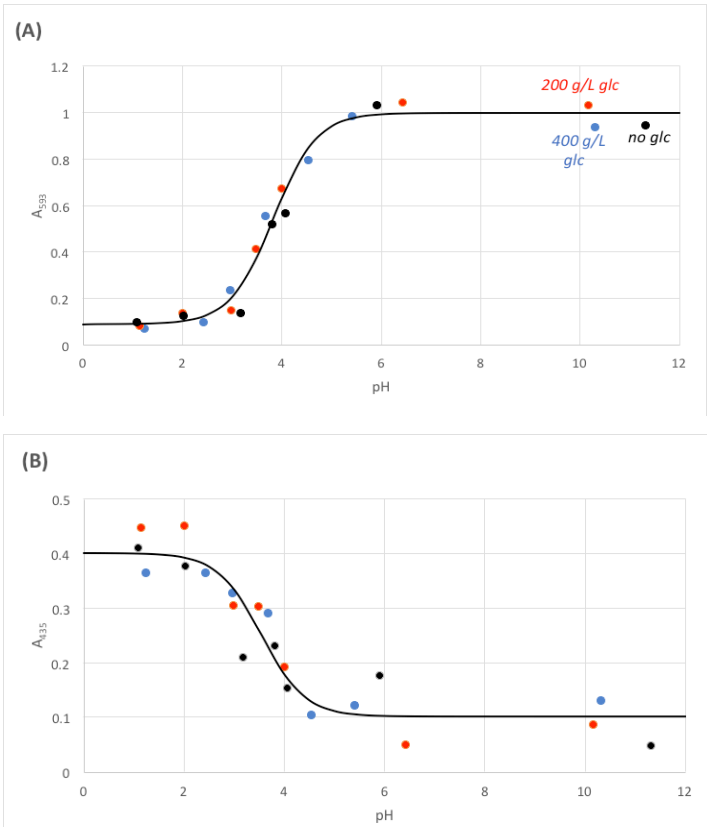

Figure 1: Spectrophotometric titration curves – NaOH was added to acidified 0.15 mM bromophenol blue in the presence of 400 g/L (blue points), 200 g/L (red points), and 0 g/L glucose (black points): (A) appearance of conjugate base, and (B) disappearance of protonated acid. Fit parameters (via nonlinear regression) are: pK_a = 3.83 ± 0.06 (A) and 3.54 ± 0.15 (B); ε_λ(molar absorptivity) = 6060 ± 200 M^{-1} (A, 593 nm, conjugate base) and 2000 ± 170 M^{-1} (B, 435 nm, protonated acid); residual absorbance = 0.089 ± 0.022 (A) and 0.102 ± 0.018 (B); R^2 = 0.98 (A) and 0.89 (B).

same titration curves. On the other hand, we noticed that in order to reach each high pH, it took more NaOH at higher glucose concentrations. This suggested to us that glucose was interacting with OH^- in such a way as to lower its activity. In order to test this, we titrated glucose into solutions of NaOH, HCl, and acetic acid to see the effect on pH.

In Figure 2 we see that added glucose has essentially no effect on the pH of HCl solutions (initial pH ≤ 4). On the other hand, for solutions that started at pH ≥ 5, glucose lowered the pH in a concentration-dependent manner, showing that glucose did in fact decrease the activity of OH^-. From the linear regression fits (Table S2), we see that for the HCl solutions, which started at pH ≤ 4, the slopes (ΔpH per kg(glucose)/L) are about zero (range: -0.4 to +1.0 L/kg glc), whereas for the NaOH solutions, which started at pH ≥ 9.5, the slopes are distinctly negative (range: -12 to -20 L/kg glc). The 1 mM acetate weak buffer started at pH 4.8 and had an intermediate negative slope (-4.5 L/kg glc). To our knowledge, this glucose-induced decline in solution pH has never before been noted in the literature (see Discussion).

To further test this glucose-induced decrease in OH^- activity, we titrated acetic acid in the presence of 0 – 200 g/L glucose (Figure 3). Data were fit to this version of the Henderson-Hasselbalch equation:

$$\text{pH} = \text{p}K_a - \log[(\text{mol acid/mol OH}^-) - 1] \quad (3)$$

where "mol acid" is the equivalence point, i.e., the amount of acid present initially, and "mol OH^-" is the amount of hydroxide added from the buret.

Three conclusions are immediately obvious from Figure 3. First, the pK_a of acetic acid, 4.51 ± 0.06 (range: 4.45 – 4.61; nonlinear regression fit parameters can be found in Table S1) is independent of glucose. Second, at the end of the titration, beyond the equivalence point, the pH is dramatically reduced by glucose (dashed lines, Figure 3). At this point, with all acetic acid in the deprotonated form, the only relevant equilibrium is the auto-ionization of water ($H_2O \rightarrow H^+ + OH^-$), whose equilibrium constant at 25°C is

$$K_w = \frac{a_{H+} \cdot a_{OH-}}{a_{H2O}} = \frac{10^{-pH} \cdot (\gamma_{OH-} \cdot c_{OH-})}{a_{H2O}} = 1.00(10^{-14}) \quad (4)$$

from which we can calculate the ratio of the hydroxide activity coefficient to the activity of water:

$$\gamma_{OH^-}/a_{H2O} = (K_w/c_{OH^-}) \cdot 10^{pH} \quad (5)$$

where c_{OH^-} is the molar concentration of OH^- in solution. We can

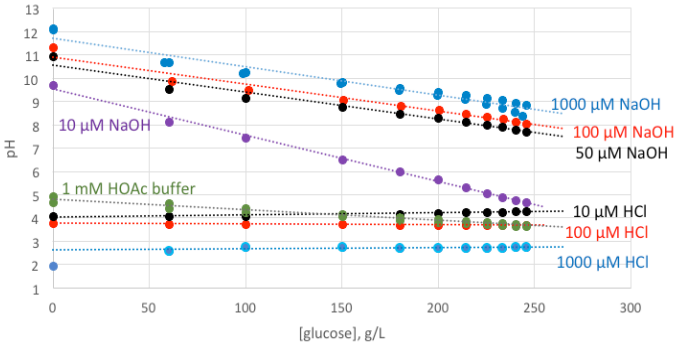

Figure 2: Effect of glucose on pH. Glucose is titrated into solutions of NaOH (10 – 1000 µM), HCl (10 – 1000 µM), and 1 mM acetate (weak buffer: 50/50 HOAc/OAc^-). Linear regression results (dotted lines) can be found in Table S2.

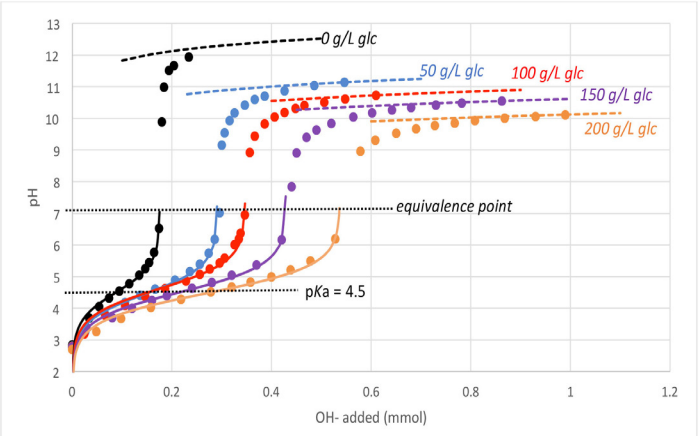

Figure 3: Titration of 13.3 mM acetic acid (0.200 mmol in 15.00 mL) with 20.0 mM NaOH, in the presence of glucose concentrations (in g/L) of 0 (black), 50 (blue), 100 (red), 150 (purple), and 200 (gold). Solid lines are data up to the equivalence point fit to Equation 3 (nonlinear regression fit parameters can be found in Table S3). Dashed lines at the end of the titration are calculated assuming K_w = $1.00(10^{-14})$ and γ_{OH^-} = 1.00 (black), 0.038 (blue), 0.013 (red), 0.0062 (purple), and 0.0020 (gold).

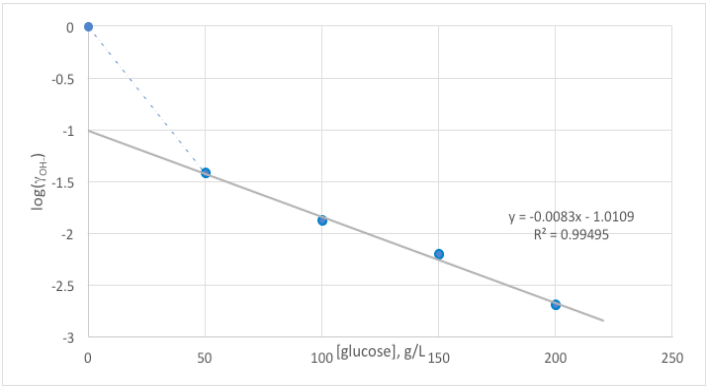

Figure 4: Decline in log(γ_{OH^-}) with glucose. γ_{OH^-} is calculated from the pH at the end of each acetic acid titration in Figure 3, using Equation 5. Linear regression for 50 – 200 g/L glucose: slope = -8.3 per kg/L; intercept = -1.01; R^2 = 0.995.

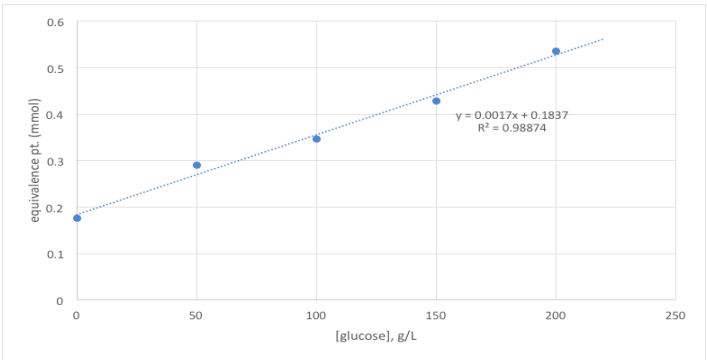

Figure 5: Increase in apparent equivalence point of acetic acid titration with glucose. Error bars are smaller than point symbols. Linear regression results: slope = 1.72 ± 0.11 mmol per kg/L; intercept = 0.184 ± 0.013 mmol; R^2 = 0.989.

see from Equation 5 that anything that causes a decrease in γ_{OH^-}/a_{H_2O} will cause the pH to fall.

At high solute concentration the activity of water falls below one, because both its mole fraction and its activity coefficient decline. At the same time, know from Figures 2 and 3 that adding glucose causes pH to fall as well. From Equation 5 we see that pH will fall only if the γ_{OH^-}/a_{H_2O} ratio declines. Thus glucose must cause a lowering of γ_{OH^-} that far outweighs the decline in a_{H_2O}. We conclude that the important effect of glucose is its lowering of γ_{OH^-}, and it is safe to ignore any effects on a_{H_2O}. The declining final pH values in Figure 3 thus suggest that glucose does lower γ_{OH^-} (Table S3). In fact, we see in Figure 4 that for 50 – 200 g/L glucose, $\log(\gamma_{OH^-})$ declines linearly with [glucose].

The final important point gleaned from Figure 3 is that the apparent equivalence point increases with glucose. (See Figure S1 for a blowup of the data in Figure 3 only up to the equivalence point). This increase occurs because glucose lowers the activity coefficient of OH^-, and the resultant lowered activity of OH^- requires a larger addition of OH^- to react with the initial 0.20 mmol of acetic acid.

In fact, we see from Figure 5 that the equivalence point increases linearly with [glucose]. The intercept, 0.184 ± 0.013 mmol, is within 8% of the expected value of 0.20 mmol (the initial amount of acetic acid titrated). The slope, 1.72 ± 0.11 mmol per kg/L glucose, shows a glucose-induced decrease in γ_{OH^-} that is substantial, but is orders of magnitude less than that observed at the end of the titration, when all acetic acid is deprotonated and the pH is much higher. The slope in Figure 4 suggests that γ_{OH^-} decreases by 8.3 orders of magnitude per kg/L glucose! Note that the hydroxide concentration is several orders of magnitude higher at the end of the titration (pH 10-12.5), compared to the equivalence point (pH 7). Clearly, the glucose-induced decrease in γ_{OH^-} is much greater at higher concentrations of hydroxide.

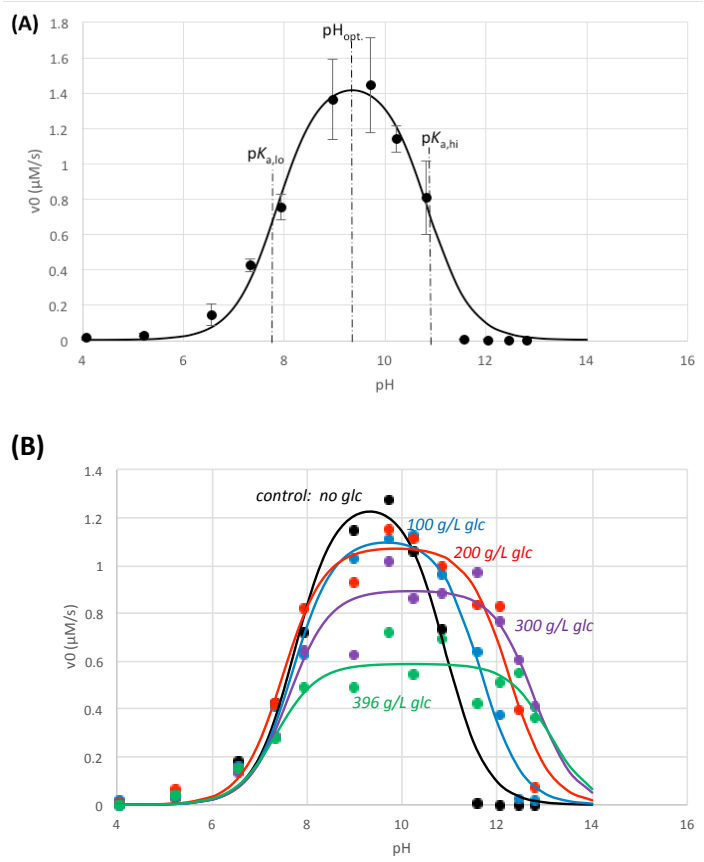

Figure 6: pH profile of YADH in the absence (A) and presence (B) of glucose; glucose concentrations (in g/L) are: 0 (black), 100 (blue), 200 (red), 300 (purple), and 396 (green). Data are fit to Equation 6 (solid curves); nonlinear regression fit parameters are listed in Table S4.

Crowding Effects on Alcohol Dehydrogenase pH Profile

Having determined that high concentrations of glucose lower the activity of hydroxide anion, we set out to test how glucose, its polymer dextran, and the protein crowding agent BSA alter the pH dependence of the activity of the enzyme alcohol dehydrogenase. Like many enzymes, YADH employs acid-base catalysis as an important part of its mechanism, such that at least two key acidic groups control activity. A side chain with a low pK_a ($pK_{a,lo}$) must be deprotonated, and another with a high pK_a ($pK_{a,hi}$) must be protonated for the enzyme to be active. This creates a bell-shaped pH profile of enzyme activity (v_0, Figure 6A), with maximal activity at a pH optimum that lies halfway between $pK_{a,lo}$ and $pK_{a,hi}$, and half-maximal activity at pH = $pK_{a,lo}$ and $pK_{a,hi}$. The dependence of v_0 on pH can be fit to the equation for the titration of a di-acid:

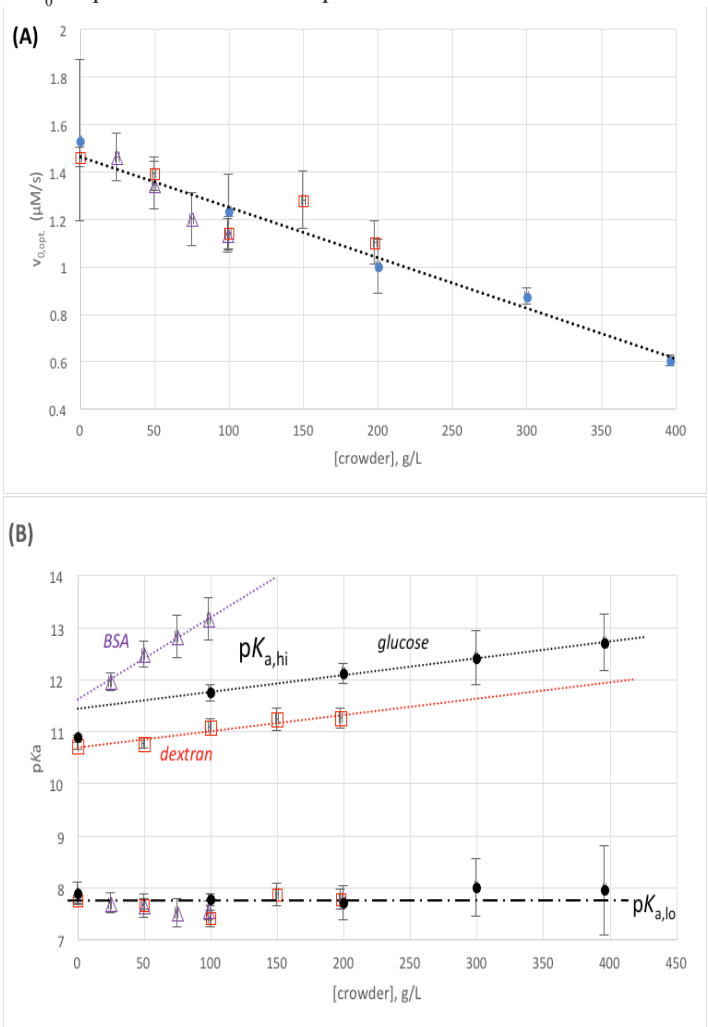

Figure 7: Effects of crowder concentration on YADH $v_{0,opt.}$ (A) and pK_a (B). Crowders are glucose (circles), dextran (squares), and BSA (triangles). Linear regression parameters: (A) slope: -2.13 ± 0.22 μM/s per kg/L; intercept: 1.46 ± 0.04 μM/s; R^2: 0.85; (B) $pK_{a,lo}$ is crowder-independent: 7.8 ± 0.3. For $pK_{a,hi}$, slope: 3.2 ± 1.0 L/kg, R^2: 0.63 for glucose; slope: 3.1 ± 0.5 L/kg, R^2: 0.92 for dextran; slope: 15.8 ± 1.2 L/kg, R^2: 0.988 for BSA.

$$v_0 = \frac{v_{0,opt.}}{1 + 10^{(pH - pK_{a,hi})} + 10^{(pK_{a,lo} - pH)}} \quad (6)$$

where v_0 is the initial reaction velocity (in μM/s), and $v_{0,opt.}$ is the velocity at optimal pH. Details of the derivation of this equation can be found in the Supporting Information for ref (7).

Regarding the effects of glucose on the pH profile of YADH, three conclusions are clear from the curves plotted in Figure 6 and the associated fit parameters listed in Table S4: $v_{0,opt.}$ declines with glucose, $pK_{a,hi}$ increases with glucose, and $pK_{a,lo}$ is unaffected by glucose. Figure 7 shows that these effects are also observed with the macromolecular crowders dextran and BSA, and the effects are linearly proportional to [crowder].

The slope of the increase of $pK_{a,hi}$ with crowder is the same for glucose and dextran, about 3 pK_a units per kg/L increase of crowder concentration, whereas the slope of the BSA line is about 5-fold higher.

BSA has an interesting protective effect on YADH activity under mildly acidic conditions, as depicted in Figure 8 and Figure 9. Below pH 7, enzyme activity declines due to the protonation of a key conjugate base side chain. In fact, the decline of v_0 to zero with acidity is independent of the concentration of dextran or glucose: The black circle points in Figure 8 are average values at each pH for all concentrations, 0 – 396 g/L. On the other hand, v_0 in the presence of BSA (open squares in Figure 8) is consistently higher than in its absence (black circles), and the difference is statistically significant (from 2.5 – 20 standard deviations). Furthermore, this enhancement of enzyme activity increases with BSA concentration up to 75 g/L. At pH 7.3 (and above), however, the difference is not statistically significant (Figure 8; from 1.2 – 1.9 standard deviations). The dependence of v_0 on BSA concentration is depicted in Figure 9. At pH < 7, in the presence of 25 g/L BSA, activity is 2 – 3 fold higher than it is in its absence, and activity rises further as BSA is added, up to 75 g/L. On the contrary, at (and above) pH 7.3 (purple points), 25 g/L BSA raises v_0 by only 14%, and it does not increase with further BSA addition.

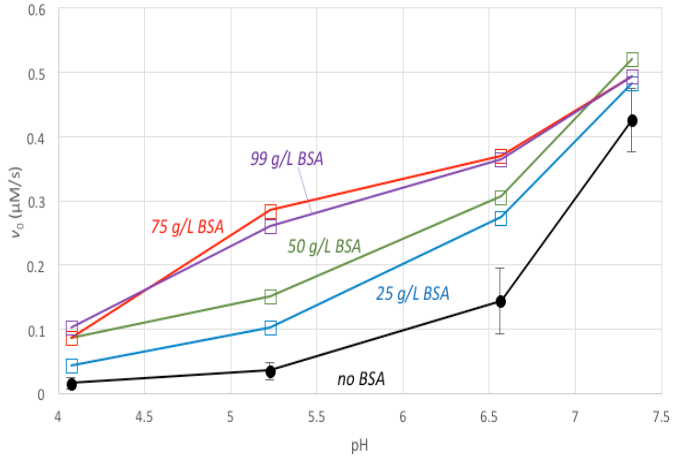

Figure 8: YADH activity under acidic conditions (pH < $pK_{a,lo}$), in the presence (squares) and absence (black circles) of BSA. The black circles are the average of all v_0 measurements in the absence of BSA, i.e., 0 – 396 g/L of glucose and dextran. Squares represent v_0 in the presence of 25 g/L (blue), 50 g/L (green), 75 g/L (red), and 99 g/L (purple) BSA.

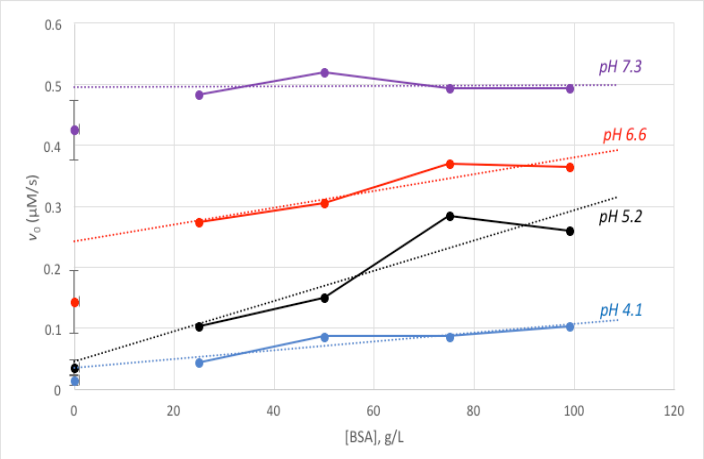

Figure 9: YADH activity below pH 7.5. The 0 g/L point at each pH is the average of all measurements in the absence of BSA, i.e., 0 – 396 g/L of glucose and dextran.

Discussion:

Glucose lowers pH

We have shown that glucose lowers the pH of hydroxide solutions (10 – 1000 μM) and 1 mM acetic acid, but not HCl solutions (10 – 1000 μM), while leaving the pK_a of acetic acid and bromophenol blue unchanged. Glucose could lower the pH of hydroxide solutions by interacting with the hydroxide anion and decreasing its activity coefficient (and leaving the molar concentration of OH^- unchanged), by reacting with hydroxide to decrease its molar concentration, or possibly both. The two most likely hydroxide/glucose chemical reactions are: nucleophilic attack to yield a hemi-acetal alkoxide (Scheme 2), and oxidation to gluconate (i.e., the "blue bottle" experiment, Scheme 3).

Hemi-acetal alkoxide formation (Scheme 2) is not expected to be appreciable for two reasons: The straight chain (2) is much less

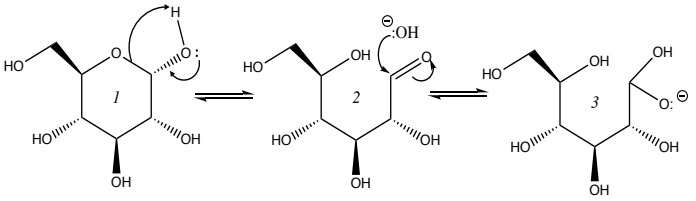

Scheme 2: Hydroxide attack on aldehyde (glucose) to give hemi-acetal.

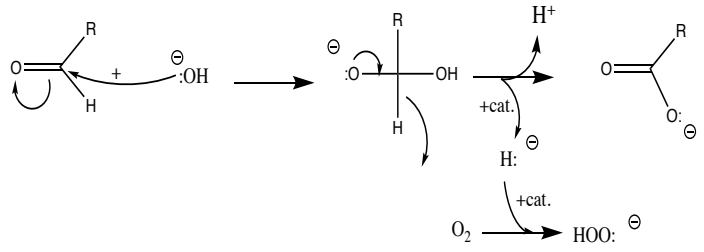

Scheme 3: Glucose oxidation to gluconate under alkaline conditions; oxidation of a second glucose would reduce the peroxide (HOO^-) to 2 OH^-, giving the net reaction: 2 RCH=O + 2 OH^- + O_2 → 2 $RCOO^-$ + 2 H_2O.

stable than the pyranose ring form (1, $\Delta G° = +5$ kcal/mol (10)), and the hemi-acetal (3) is less stable than the aldehyde (2, $\Delta G° \approx +1$ kcal/mol (11)). Even though high glucose concentration will push this reaction forward, our highest concentration (400 g/L, 2.2 M) would supply a driving force of only 0.5 kcal/mol at 25 °C.

Dioxygen oxidation of glucose to gluconate (Scheme 3) is quite spontaneous, as readily observed in the well-known "blue bottle" classroom demonstration (12,13). However, this reaction generally requires hydroxide concentrations ≥ 0.1 M, and even then, only occurs at appreciable rates in the presence of two-electron redox mediator dyes (13,14). For these reasons, we believe it most likely that glucose lowers the activity of hydroxide (and thus lowers pH) not by reacting chemically with it, but by interacting with it so as to lower its activity coefficient.

This ability of glucose to lower γ_{OH-} appeared at two points in the acetic acid titrations depicted in Figure 3, at the equivalence point and at the end of the titration. Comparing the slope in Figure 4 (-8.3 L/kg, $\log(\gamma_{OH-})$ vs. [glucose]) to that in Figure 5 (1.7 mmol per kg/L, equivalence point vs [glucose]) shows that this effect is extremely concentration-dependent. At the end of the titration, where hydroxide concentration is several orders of magnitude higher than it is at the equivalence point, glucose causes a much greater lowering of γ_{OH-} .

Although to our knowledge, this is the first report in the literature demonstrating the tendency of glucose to lower γ_{OH-}, there are a number of reports showing that adding glucose caused internal pH to decline in various cells and organelles (15-17). These authors interpreted the pH decrease of about 0.5 pH units to the addition of glucose triggering the fermentative production of metabolic acids. Although this is certainly possible, we note here that this pH decline can be at least partially (and perhaps fully) accounted for by the glucose-induced pH (and γ_{OH-}) declines that we depict in Figure 2.

Glucose inhibits YADH activity and raises $pK_{a,hi}$

Alcohol dehydrogenase, like almost all NAD-linked dehydrogenases, is somewhat unusual for a Michaelis-Menten enzyme in that its rate-limiting step is product (NADH) release (18).This is not totally unexpected, because substrate (NAD^+) binding to the nucleotide binding domain is accompanied by a significant open to closed conformational change [19], where the open state of YADH is more compact than the closed conformation (20). Because product release must reverse the changes during substrate binding (i.e., E_{closed}•NADH → E_{open} + NADH), excluded volume, which favors the more compact open state, should speed up the rate-determining product release step and increase enzyme activity (8).

On the other hand, it is also important to consider the fact that high concentrations of crowding agents often increase solution viscosity.[8] Higher viscosity will impede the diffusion of the product away from the binding site, and enhance rebinding (21). Increased viscosity could also hinder any enzyme conformational changes that involve significant volume fluctuations (22-24). Either of these two viscosity effects would slow down YADH's rate-determining product release step (8).

We show in Figure 7A that $v_{0,opt.}$ decreases by ≈ 2 μM/s per kg/L of added crowder, which matches the dextran inhibition seen by Schneider et al (40% inhibition at 300 g/L [8]), but is somewhat less than the inhibition that they observed with glucose (8,9). Schneider et al showed that glucose and dextran at equal concentrations had the same effect on solute diffusion coefficients, concluding that crowder inhibition of YADH stems from the viscosity-induced inhibition of product diffusion away from the binding site (8). Our results showing that glucose, dextran, and BSA all fall on the same line in Figure 7A agree with this conclusion.

Structural studies have associated specific amino acid side chains in ADH with $pK_{a,lo}$ and $pK_{a,hi}$ (25,26). $Histidine_{51}$, which begins a proton transfer chain that includes NAD^+-ribose-OH and ser/thr_{48}-OH, and ends with the substrate ethanol-OH (middle of Figure 10), is believed to titrate with $pK_{a,lo} \approx 7.5$. The ribose-OH proton hydrogen-bonds to the histidine imidazole nitrogen, and therefore the latter must be deprotonated in order to activate the proton transfer chain and bind both the NAD^+ and the ethanol substrates. $Lysine_{228}$-NH_3^+, which forms a hydrogen bond with a hydroxyl oxygen of the NAD^+-ribose-OH substrate (25,26) (top of Figure 10), could account for $pK_{a,hi} \approx 10.6$; it must be protonated to optimize NAD^+ binding. Alternatively, the decrease in activity at high pH could be due to denaturation of the enzyme (note that activity declines to zero for pH > 11.5, Figure 7A).

In Figure 7B we show that whereas crowding has no effect on $pK_{a,lo}$ of YADH, it increases $pK_{a,hi}$. The two amino acid side chains identified with these pK_a values, his_{51} and lys_{228}, respectively, both form part of the nucleotide binding domain, as they both hydrogen-bond to the NAD^+ substrate. At first glance it would thus seem surprising that crowding could have such disparate effects on the two side chains. However, NAD^+ is a large molecule, and the two side chains interact with ribose-OH groups on different ends of the molecule: His_{51} hydrogen-bonds to the ribose-OH adjacent to the

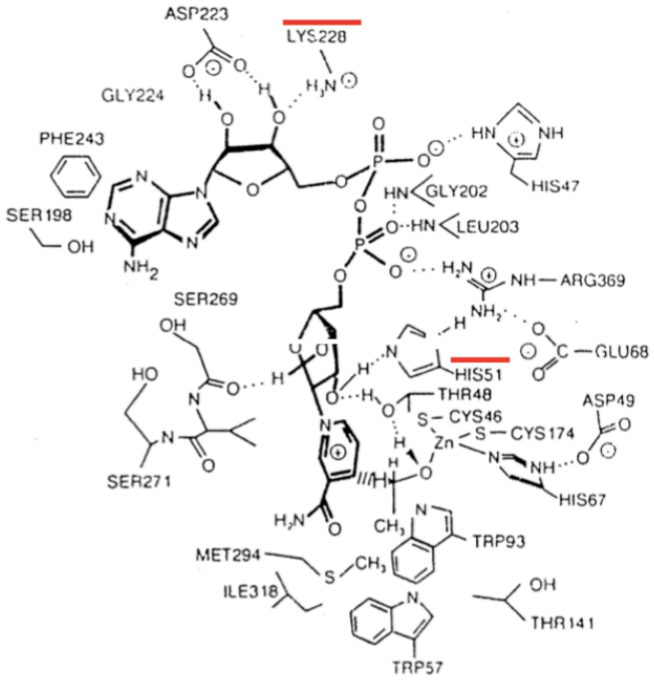

Figure 10: YADH active site, showing side chains that bind NAD^+ (in bold). His_{51} ($pK_{a,lo}$) and lys_{228} ($pK_{a,hi}$) are marked in red. Modified from ref (26). .

nicotinamide group (middle of Figure 10), whereas lys_{228} interacts with the ribose-OH adjacent to the adenine group (top of Figure 10).

Our results suggest that crowding by dextran, glucose, and BSA leaves the environment around his_{51} unchanged, whereas the environment around lys_{228} is altered to stabilize the protonated lys_{228}-NH_3^+ and thus increase its pK_a. This could occur by bringing closer to lys_{228} either a full negative charge (e.g., from the nearby $aspartate_{223}$ side chain, top of Figure 10) or a partial negative charge (e.g., from the nearby pyrophosphate P=O oxygen, Figure 10). The fact that both glucose and dextran (and even BSA at concentrations ≤ 50 g/L) have this effect suggests that the conformational change is not due to excluded volume, but rather to either a chemical interaction or to the crowder-induced increase in viscosity. Alternatively, the increase in $pK_{a,hi}$ could be due to a protective effect of crowding against alkaline-induced denaturation. Further studies on the effects of crowding on enzyme pH-stability will allow us to distinguish between these two explanations.

Finally, while none of the crowding agents altered $pK_{a,lo}$, Figure 8 and Figure 9 show that BSA activated YADH at pH values below 7.5. At pH 6.6, BSA raised $v_{0,opt.}$ about two-fold, in a concentration-dependent manner; at pH 5.2 and 4.1, the increase was about three-fold. Because $pK_{a,lo}$ remained the same, BSA could not have directly influenced the protonation state of his_{51}. Instead, it must have favored the more compact open conformation of YADH, thus speeding up the rate-determining NADH release step at these low pH values. Above pH 7 this effect was greatly attenuated, and was not concentration-dependent. These enhanced effects of BSA on low-pH YADH activity and on the increase of $pK_{a,hi}$ (Figure 7B) bear further study.

Conclusion and Future Studies

From titrations of Bromophenol blue and acetic acid we determined that glucose interacts with hydroxide anion so as to dramatically lower its activity coefficient. This effect is dependent on the concentrations of both glucose and hydroxide. Unfortunately, we did not have time to test the effects of the macromolecular crowders dextran and BSA on pH and pKa. The results of such studies would be of great interest. Regarding the enzymatic activity of YADH, glucose, dextran, and BSA all lowered $v_{0,opt.}$, left $pK_{a,lo}$ unchanged, and raised $pK_{a,hi}$. These effects are not due to excluded volume, but rather to crowder-YADH chemical interactions and/or crowder-induced viscosity increase. BSA has some interesting effects on YADH activity that bear further study.

Acknowledgments

We wish to acknowledge Kristin Slade for her assistance with our experimental and theoretical questions, and for her suggestions regarding this manuscript.

References

1. Zimmerman SB, Trach SO, *Journal of molecular biology,* **1991**, 222:599–620.
2. Fulton AB, Cell, **1982**, 30:345–347.
3. Silverstein TP, Slade K., *Journal of Chemical Education*, **2019**, 96:2476–2487.
4. Kuznetsova IM, Zaslavsky BY, Breydo L, et al. *Molecules*, **2015**, 20:1377–1409
5. Kuznetsova IM, Turoverov KK, Uversky VN, *International journal of molecular sciences*, **2014**,15:23090–23140
6. Gnutt D, Ebbinghaus S., *Biological chemistry* **2016**, 397:37–44
7. Silverstein TP. *Journal of Chemical Education*, **2016**, 93:963–970
8. Schneider SH, Lockwood SP, Hargreaves DI, et al., *Biochemistry* **2015**, 54:5898–5906
9. Wilcox AE, LoConte MA, Slade KM., *Biochemistry*. **2016**, 55:3550–3558
10. Zubay, Geoffrey L. *Biochemistry*, 4th ed. Wm. C. Brown, Dubuque, IA; , **1998**, p. 285
11. Bell RP, McDougall AO. *Transactions of the Faraday Society* **1960**, 56:1281–1285
12. Vandaveer IV WR, Mosher M, *Journal of Chemical Education* **1997**, 74:402
13. Limpanuparb T, Ruchawapol C, Pakwilaikiat P, Kaewpichit C. *ACS omega* **2019**, 4:7891–7894
14. Sowden JC, Schaffer R. *Journal of the American Chemical Society* **1952**, 74:499–504
15. Jähde E, Rajewsky MF. *Cancer research* **1982**, 42:1505–1512
16. Volk T, Jähde E, Fortmeyer HP, et al *British journal of cancer* , **1993**, 68:492–500
17. Dellian M, Helmlinger G, Yuan F, Jain RK. *British journal of cance*r **1996**, 74:1206–1215
18. Nagel ZD, Klinman JP., *Chemical reviews*, **2006**, 106:3095–3118
19. Raj SB, Ramaswamy S, Plapp BV. *Biochemistry* **201**4, 53:5791–5803
20. Cho Y-K, Northrop DB. *Biochemistry* ,**1999**, 38:7470–7475
21. Olsen SN.*Thermochimica Acta*, **2006**, 448:12–18
22. Sierks MR, Sico C, Zaw M., *Biotechnology progress* **1997**, 13:601–608
23. Uribe S, Sampedro JG. *Biological procedures online* **2003**, 5:108–115
24. Demchenko AP, Rusyn OI, Saburova EA.*Biochimica et Biophysica Acta (BBA)-Protein Structure and Molecular Enzymology* **1989**, 998:196–203
25. Hammes-Schiffer S, Benkovic SJ. *Annu Rev Biochem* **2006**, 75:519–541
26. Trivic S, Leskovac V. *J Serb Chem Soc* **2000**, 65:207–227

Appendix

Table S1: Buffers used for the YADH pH profile.

pH	buffer
4.073 ± 0.021	Acetic acid
5.227 ± 0.015	Acetic acid
6.567 ± 0.015	KH_2PO_4
7.327 ± 0.006	KH_2PO_4
7.94 ± 0.05	Tris-NH_3Cl
8.97 ± 0.03	Tris-NH_3Cl
9.723 ± 0.005	glycine
10.237 ± 0.006	glycine
10.83 ± 0.06	glycine
11.570 ± 0.010	Na_2HPO_4
12.047 ± 0.006	Na_2HPO_4
12.46 ± 0.04	Na_2HPO_4
12.807 ± 0.021	Na_2HPO_4

Table S2: Linear regression results for data in Figure 2.

	Slope (ΔpH per kg glc/L)	Intercept (pH w/o glc)	R^2
1000 µM NaOH	-12.4 ± 0.6	11.74 ± 0.11	0.953
100 µM NaOH	-11.7 ± 0.8	10.92 ± 0.14	0.962
50 µM NaOH	-11.6 ± 0.7	10.57 ± 0.14	0.965
10 µM NaOH	-19.7 ± 0.4	9.95 ± 0.07	0.997
1 mM HOAc	-4.52 ± 0.20	4.79 ± 0.04	0.964
10 µM HCl	1.03 ± 0.13	4.014 ± 0.023	0.88
100 µM HCl	-0.396 ± 0.011	3.7784 ± 0.0021	0.993
1000 µM HCl	0.49 ± 0.24	2.63 ± 0.05	0.35

Table S3: Nonlinear regression fit parameters for acetic acid titration in Figure S1. γ_{OH^-} is calculated from the final data point of each curve in Figure 3.

[glucose], (g/L)	pK_a	Equivalence point (mmol)	R^2	γ_{OH^-}
0	4.50 ± 0.03	0.1755 ± 0.0004	0.994	1.0
50	4.45 ± 0.03	0.2909 ± 0.0012	0.995	0.038
100	4.61 ± 0.05	0.3473 ± 0.0006	0.98	0.013
150	4.50 ± 0.03	0.4287 ± 0.0018	0.996	0.0062
200	4.47 ± 0.03	0.5371 ± 0.0024	0.993	0.0020

Table S4: Nonlinear regression fit parameters for YADH pH profiles in Figure 6.

[glucose], g/L	$pK_{a,lo}$	$pK_{a,hi}$	$v_{0,opt.}$ (µM/s)	R^2
0 (Fig. 6A)	7.86 ± 0.08	10.84 ± 0.08	1.50 ± 0.06	0.955
0 (Fig. 6B)	7.74 ± 0.08	10.91 ± 0.08	1.29 ± 0.05	0.985
100	7.70 ± 0.09	11.65 ± 0.08	1.12 ± 0.04	0.98
200	7.49 ± 0.13	12.25 ± 0.11	1.08 ± 0.05	0.96
300	7.61 ± 0.16	12.78 ± 0.15	0.90 ± 0.05	0.94
396	7.35 ± 0.21	13.10 ± 0.25	0.59 ± 0.04	0.89

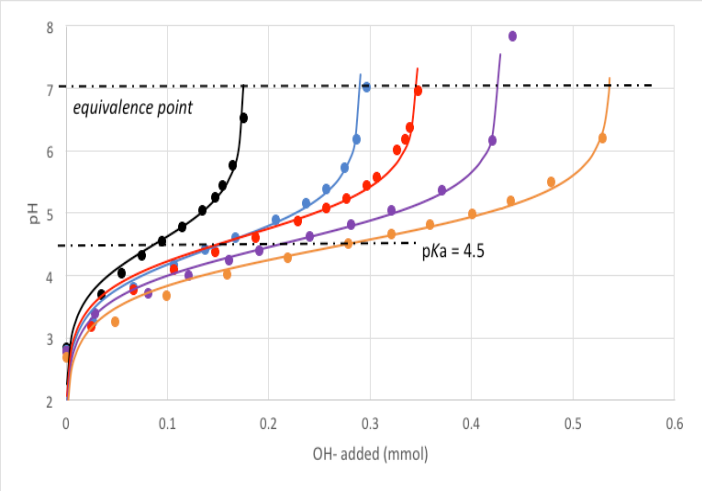

Figure S1: Titration of 13.3 mM acetic acid (0.200 mmol in 15.00 mL) with 20.0 mM NaOH, in the presence of glucose concentrations (in g/L) of 0 (black), 50 (blue), 100 (red), 150 (purple), and 200 (gold). This titration up to the equivalence point is a subset of data from Figure 3; data are fit to Equation 3 (solid lines); nonlinear regression fit parameters can be found in Table S1.